International Journal of GEOMATE, June, 2026 Vol.30, Issue 142, pp.110-117
ISSN: 2186-2982 (P), 2186-2990 (O), Japan, DOI: https://doi.org/10.21660/2026.142.g14298
Geotechnique, Construction Materials and Environment

SEISMIC AND TSUNAMI VULNERABILITY ASSESSMENT OF THE SHELTER SCHOOL BUILDING IN PADANG CITY, INDONESIA

*Fauzan[1], Heriansyah Putra[2], Achmad Basuki[3], Louise K. Comfort[4], and Zawil Huda[5]

[1,5]Department of Civil Engineering, Faculty of Engineering, Universitas Andalas, Indonesia
[2]Department of Civil and Environmental Engineering, IPB University, Bogor, Indonesia
[3]Department of Civil Engineering, Sebelas Maret University, Surakarta, Indonesia
[4]Center for Disaster Management, University of Pittsburgh, Pittsburgh, United States of America

*Corresponding Author, Received: 30 June 2025, Revised: 01 March 2026, Accepted: 05 March 2026

ABSTRACT: West Sumatra Province is one of the most earthquake and tsunami-prone areas in Indonesia. Currently, tsunamis pose a serious threat to coastal areas in Padang City, as they can damage public buildings, including schools. Consequently, it is essential to assess the vulnerability of school buildings in coastal areas of West Sumatra. One of the school buildings that can function as a shelter in the city coastline area of Padang is SDN 23 Padang. In this study, vulnerability analysis is conducted using the development of a fragility curve. The seismic fragility curve was developed by analyzing the maximum structural displacement under various earthquake accelerations, obtained through dynamic response simulations and non-linear time history analysis scaled with the Incremental Dynamic Analysis (IDA) approach. The limit states were defined according to ATC-40 criteria and further classified using the HAZUS framework. For tsunami hazards, the fragility curve was derived from the peak displacement responses corresponding to different inundation depths. The seismic vulnerability assessment indicates a progressive probability distribution at a 0.6 g peak ground acceleration, where the likelihood of slight and moderate damage of the building reaches 100%, while extensive damage is approximately 74%, and the probability of collapse remains negligible. In contrast, the tsunami vulnerability assessment indicates that at an inundation height of 5 m, the likelihood of slight and moderate damage to the building is certain, the probability of extensive damage is 96%, and complete structural failure has a probability of approximately 10%.

Keywords: Shelter, Tsunami, Vulnerability Assessment, Fragility Curve, Padang

1. INTRODUCTION

West Sumatra is recognized as one of the Indonesian provinces most exposed to natural disasters, particularly earthquakes and tsunamis [1]. This vulnerability arises because the region is influenced by three primary seismic sources: the Sumatra Fault Zone, the subduction zone where the Indo-Australian plate converges with the Eurasian plate, and the Mentawai Fault Zone [2,3]. Several strong earthquakes have struck the area, including the significant event on September 30, 2009, in Padang City, which recorded a magnitude of 7.6 on the Richter scale [4]. Although it did not cause a tsunami, the devastating earthquake that hit the coast of West Sumatra killed around 1,700 people and damaged more than 200,000 buildings [4].

Padang City, the provincial capital of West Sumatra, is categorized as a zone with very high tsunami risk [5–8]. This condition requires that essential public infrastructures, including hospitals, government offices, sports facilities, and educational buildings, be designed with specific engineering considerations to reduce the potential for severe damage or structural failure caused by earthquake and tsunami forces [9–11]. One of the public facilities in Padang City, as an educational facility, is the SDN 23/24 Padang building.

SDN 23 Padang was constructed in 2013, and the school building is owned by the local government. The school building consists of three buildings, which are three-story and two-story reinforced concrete buildings. An examination of the Detail Engineering Design (DED) documents revealed that the school was constructed without considering tsunami loading. Its location, which is very near the shoreline, increases the potential risk when a major earthquake accompanied by a tsunami occurs [12]. Hence, it is essential to conduct a comprehensive structural evaluation to determine the building's capacity to withstand both regular service loads and tsunami-induced forces, as well as to analyze the potential impacts of such loads on the SDN 23 Padang facility.

With the recent updates to seismic design codes and the growing number of reinforced concrete (RC) school buildings in Indonesia, there is a pressing need to perform vulnerability assessments for educational facilities located in disaster-prone regions. Such analyses are crucial to estimate potential losses and evaluate the structural performance of these buildings when subjected to earthquake and tsunami forces, in line with the latest regulatory requirements.

2. RESEARCH SIGNIFICANCE

This study discusses the assessment of

vulnerability due to earthquakes and tsunamis for an educational building in earthquake- and tsunami-prone areas in accordance with applicable regulations. The purpose of employing fragility curve analysis is to quantify potential losses resulting from structural damage under earthquake and tsunami loads, in accordance with current codes. The findings of this research are expected to serve as a valuable reference for evaluating the vulnerability of school facilities that also serve as vertical evacuation shelters, particularly in regions exposed to strong seismic activity and potential tsunami events.

3. METHODOLOGY

3.1 Existing Building Data

The object of this study is the school building of SDN 23 Padang, which is located on Jalan Veteran No. 90 (Fig.1), Padang City, Indonesia, about 474 meters away from Padang beach (Fig.2). Tables 1 and 2 show the building's cross-sectional dimensions.

Fig.1 Front view of SDN 23 Padang

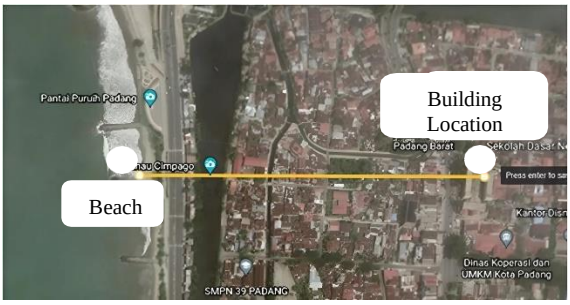

Fig.2 Location of SDN 23 Padang building from the beach

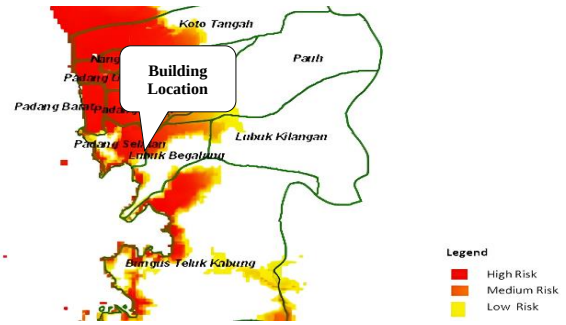

Fig. 3. Tsunami-Prone Zone of Padang City

Based on the tsunami-prone zone map of Padang city shown in Fig. 3, the SDN 23 Padang building is located in the West Padang area, which is an area with a high level of vulnerability (High Risk Zone) to tsunamis [13].

Table 1. Dimensions of the cross-section of the SDN 23 Padang column.

Floor	ColumnCode	Dimension	
		Height (mm)	Width (mm)
1	C4	450	450
2	C5	350	350
3	C6	450	350

Table 2. Beam cross-sectional dimensions

Floor	BeamCode	Dimension	
		Height (mm)	Width (mm)
1	1G1	700	300
2	1G2	550	300
3	1G3	500	450
1	2G1	700	300
2	2G2	500	300
3	2G3	450	450
1	RG1	700	300
2	RG2	500	300
3	RG3	450	350

3.2 Structural Modeling

Structural modeling was performed using ETABS V21.1.1 software, as shown in Fig.4.

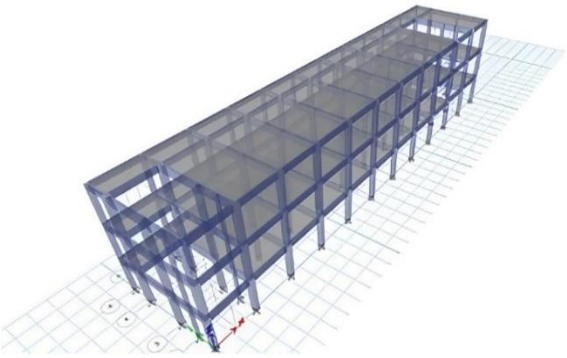

Fig.4 3D modeling structure of the existing building

3.3 Loading Analysis

3.3.1 Vertical load

The vertical loading on the structure consists of dead load (DL) and live load (LL), which represents the functional demands of the evacuation facility. Dead loads are automatically generated in ETABS and account for the self-weight of structural elements such as slabs, beams, and columns. Meanwhile, live loads are defined as refugee occupancy loads, determined in accordance with the Indonesian standard SNI 1727:2020, with values of 1.92 kN/m² for classrooms and 4.79 kN/m² for corridors [14].

3.3.2 Horizontal load

The horizontal loading is represented by earthquake forces, defined according to SNI 1726:2019 [15]. The building is classified under risk category IV with an importance factor (Ie) of 1.5. Since the structure applies a special moment-resisting composite steel–concrete frame, the corresponding seismic design parameters are a response modification factor (R) of 8, an overstrength factor (Ω) of 3, and a deflection amplification factor (Cd) of 5.5. In addition, the site coefficient parameters include Ct = 0.0466 and x = 0.9. The design spectral acceleration values, SDS = 0.75 and SD1 = 0.7851, were adopted for Padang City and subsequently used in the spectral response analysis (Fig.5)

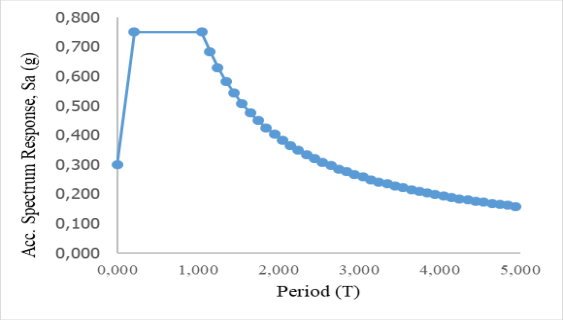

Fig. 5 Padang City's spectrum response with soft soil

3.3.3 Ground motion record

The seismic load will also be analyzed using the time-history method to ensure that the selected ground motion acceleration is compatible with the location of the structure. The applied earthquake acceleration data are displayed in Table 3.

Table 3. Data on earthquake acceleration

Name	Data	Unit
Chichi-X	0.580	g
Chichi-Y	0.640	g
Kobe-X	0.610	g
Kobe-Y	0.640	g
Superstition Hills-X	0.640	g
Superstition Hills-Y	0.636	g

3.3.4 Tsunami load

According to FEMA P-646-2019 [16], these forces must be considered comprehensively when designing buildings in tsunami-prone areas, particularly those designated for vertical evacuation [17]**.** The tsunami loads generally include:

1. Hydrostatic Force

Hydrostatic force is a lateral force resulting from water pressure against submerged parts of the structure. Its magnitude depends on water depth and the area exposed. The hydrostatic force can be estimated using Eq. (1).

$$Fh = 0.5\ \rho_s\ g\ b\ {h_{max}}^2 \quad (1)$$

2. Buoyancy Force

Buoyancy forces are an upward force acting on partially or fully submerged structures. It can potentially cause uplift or overturning, especially in lighter elements. Buoyancy force can be computed using Eq. (2).

$$Fb = \rho_s\ g\ V \quad (2)$$

3. Hydrodynamic Force

Hydrodynamic force is caused by water flowing past the structure, combining pressure and drag effects. This force depends on flow velocity, depth, and surface geometry. Hydrodynamic force can be computed using Eq. (3).

$$Fh_d = 0.5\ \rho_s\ cd\ b\ (hu^2)_{max} \quad (3)$$

4. Impulsive Force

Impulsive force is a sudden impact resulting from the leading edge of the tsunami wave striking the structure and is often more severe than steady-state forces. The impulsive force of the building is 1.5 times the hydrodynamic force.

5. Debris Load

Debris load results from the accumulation of floating materials carried by the tsunami flow, which is modeled as an additional hydrodynamic force. The magnitude of this force is influenced by the thickness of the debris layer acting against the structure, and its calculation is expressed in Eq. (4).

$$F_{dm} = 0.5\ \rho_s\ cd\ Bb\ (hu^2)_{max} \quad (4)$$

6. Impact Load

Impact loads arise when floating objects carried by tsunami currents, such as logs, small vessels, building fragments, or other debris, collide with structural components. These sudden collisions can generate significant localized forces that must be considered in the overall design of tsunami-resistant buildings. Impact load can be calculated using Eq. (5).

$$Fi = 1.3\ \mu_{max}\sqrt{k + md\ (1 + c)} \quad (5)$$

7. Additional Gravity Load

Additional gravity load as tsunami water accumulates on floors adds substantial vertical loads, especially when drainage is delayed. Additional gravity load can be calculated using Eq. (6).

$$F_i = \rho_s\ g\ h_r \quad (6)$$

8. Uplift Force on Elevated Floors

Uplift forces on upper floor levels develop when tsunami water penetrates beneath slabs or deck

structures, generating upward pressure that can lift these elements. This phenomenon introduces additional challenges in vertical load design, and its magnitude is determined using Eq. (7).

$$F_u = 0.5\, C_u\, \rho_s\, A_f\, {U_v}^2 \quad (7)$$

Where:
ρ_s = tsunami volume weight, g = represents gravitational acceleration, b = width of the structural surface exposed to fluid pressure, h_{max} = maximum inundation depth measured from the base of the wall, V = volume of water below the maximum inundation, cd = drag coefficient, h = flow depth, u = flow velocity, U_{max} = peak flow velocity associated with the maximum inundation volume, $h_r = h_{max} - 1^{st}$ floor height, C_u = uplift coefficient, U_v = hydrodynamic uplift force.

Each of these load types contributes to the overall structural demand and should be included in load combinations when performing tsunami vulnerability assessments. The calculation of these forces follows specific formulations provided in FEMA standards, taking into account fluid properties, structural dimensions, and inundation characteristics. In this research, the tsunami load calculations encompass several components, including hydrostatic, buoyancy, hydrodynamic, impulsive forces, debris impact, and additional forces from debris accumulation, which were derived based on the tsunami run-up design and hazard map of Padang City.

3.3.5 Load combination

Structural loads combination refers to the New Indonesian Seismic Code (SNI 1726:2019) [15]:
1. 1.4 D
2. 1.2 D + 1.6 L + 0.5 (Lr or R)
3. 1.2 D + 1.6 (Lr or R) + (L or 0.5 W)
4. 1.2 D + 1.0 W + L + 0.5 (Lr or R)
5. 0.9 D+ 1.0 W
6. 1.2 D + EV + EH + L
7. 0.9 D - EV + EH

A combination of tsunami loads acting on the structure refers to FEMA P-646 [16]:
1. 1.2 DL + 1.0 TS +1.0 Lref + 0.25 LL
2. 0.9 DL + 1.0 TS

Where:
DL = Dead load, LL = Live load, Lr = Live load on the roof, W = Wind load, R = Rain load, EQX = Earthquake load in X direction, EQY = Earthquake load on Y-direction, EV = 0.2SDS x D, EH = Rho x QE, Rho = 1.3 (Redundancy), Ts = Tsunami load, Lref = Live load in refuge area.

3.3.6 Incremental Dynamic Analysis (IDA)

Following the completion of structural modeling, the subsequent step involves inputting the earthquake history data. A dynamic time history analysis is then conducted incrementally, gradually escalating the earthquake intensity scale. In the analysis, scale factors are gradually increased in steps of 0.2 to define the range of successive load intensifications. The simulation results produced displacement responses in both the x and y axes, which were then used to determine the drift ratio. This parameter is fundamental for developing the Incremental Dynamic Analysis (IDA) curve [18].

3.3.7 Hazus Damage Classification Criteria

The HAZUS methodology, developed by FEMA, provides a widely accepted framework for classifying structural damage levels in vulnerability and risk assessments [19,20]. These damage classifications are particularly relevant to evaluating potential losses due to earthquakes and tsunamis, and are instrumental in developing fragility curves.

1. Slight Damage (RR)

Slight damage (RR) is characterized by cosmetic or minor non-structural issues. This includes small cracks in plaster, dislodged ceiling panels, or minor displacement of non-load-bearing partitions. Structural integrity remains unaffected, and repairs are minimal.

2. Moderate Damage (RS)

Moderate Damage (RS**)** indicates light structural impairment alongside more evident non-structural damage. Examples include cracked masonry, deformation in non-critical structural elements, or loss of functionality in internal systems. The building may still be usable, but would require repair before continued operation.

3. Extensive Damage (RB)

Extensive damage (RB) represents significant degradation in structural components, such as buckling of columns or yielding of beams. At this stage, the building's capacity to resist further loading is diminished, potentially making it unsafe for occupancy without major rehabilitation.

4. Complete Damage (Collapse)

Complete damage (collapse) describes full or nearly total structural failure, often involving the collapse of key load-bearing elements. The building is considered a total loss, posing severe life-safety risks and requiring complete reconstruction.

These standardized categories are vital for interpreting the performance of buildings under disaster scenarios and serve as the backbone for decision-making in mitigation planning, emergency response, and design improvements.

3.3.8 Fragility Curve

The development of fragility curves in this study was carried out through an analytical approach that

relates the probability of a structure reaching certain damage states to increasing hazard intensity levels. A fragility curve illustrates how the likelihood of structural damage evolves as the severity of seismic or tsunami loading increases [21]. In this research, the Probabilistic Seismic Demand Model (PSDM) with a cloud method was applied, where regression analysis was performed between the intensity measure (IM) of the hazard and the engineering demand parameter (EDP), such as structural drift.

The fragility function is expressed as a lognormal cumulative distribution, which estimates the probability of exceeding a particular damage state for a given hazard intensity. For seismic analysis, peak ground acceleration (PGA) served as the IM, while for tsunami evaluation, inundation depth was used as the intensity measure. The key statistical parameters, including mean and standard deviation, were obtained by fitting the analysis results to a lognormal distribution.

To generate the required data, pushover analysis was employed to determine yield displacement, while non-linear time history analysis provided maximum drift values. These results were then combined to calculate structural ductility, which served as the basis for deriving fragility curves. This procedure enables the identification of vulnerability trends and quantification of structural performance, particularly in evaluating the effectiveness of retrofitting strategies under combined seismic and tsunami scenarios.

3.3.9 Seismic fragility curve

From the structural analysis conducted using the Incremental Dynamic Analysis (IDA) method, a series of IDA curves were generated based on the different earthquake records applied as loading inputs. These IDA curves were then evaluated probabilistically through the fragility function to develop fragility curves. In this research, the definition of limit states was adopted from ATC-40 [22].

The seismic fragility curve depicts the relationship between the probability of the degree of structural damage and the ground motion intensity measure (IM). The IM used in the seismic fragility curve is peak ground acceleration (PGA). The parameters used in the calculation of the seismic fragility curve are obtained from the results of pushover analysis in the form of drift yield values and from the results of non-linear time history analysis in the form of maximum drift values with incremental dynamic analysis.

The fragility curve can be further analyzed based on the function derived by Keith Porter [23] through a normal distribution approach as follows:

$$P = \phi \frac{ln(\frac{x}{\theta})}{\beta} \quad (8)$$

$$\boldsymbol{v = \sigma/\mu} \quad (9)$$

$$\boldsymbol{\theta = \frac{\mu}{\sqrt{(1+v^2)}}} \quad (10)$$

$$\boldsymbol{\beta = \sqrt{(\ln(1+v^2))}} \quad (11)$$

Where:

P represents the probability of structural damage, ϕ denotes the standard normal distribution function, and x is the ground motion parameter expressed as PGA (g). The symbol θ indicates the median demand capacity in terms of PGA (g), while β refers to the overall structural uncertainty. The parameter v is the coefficient of variation for the damage threshold, σ is the standard deviation of the damage limit, and μ corresponds to its mean value.

3.3.10 Tsunami fragility curve

The tsunami fragility curve was derived by evaluating the maximum structural displacements produced under different levels of tsunami inundation depth, as presented in Table 4. The overall procedure for developing both seismic and tsunami fragility curves is illustrated in the flowchart provided in Fig. 6.

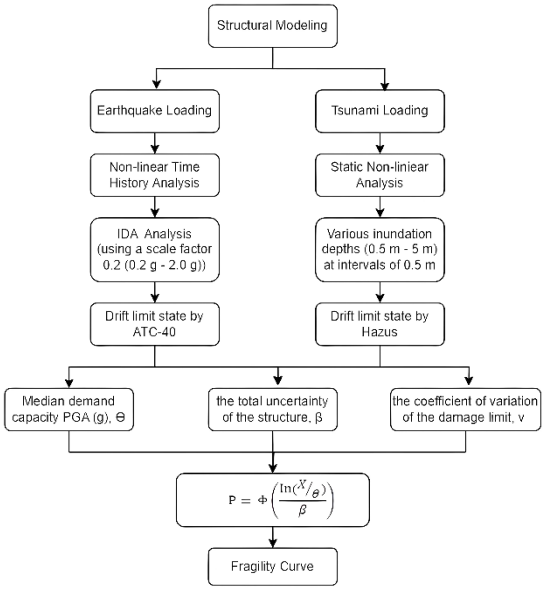

Fig.6 Flowchart of seismic and tsunami fragility curve development

Table 4. Damage states limit of the tsunami fragility function by Hazus.

Damage states	Drift damage index HAZUS (%)
Slight	< 0.20
Moderate	0.20 – 0.50
Extensive	0.50 – 1.20
Complete	1.20 – 2.80

4 RESULTS AND DISCUSSION

4.1 Incremental Dynamic Analysis

The Incremental Dynamic Analysis (IDA) produced structural response data in the form of acceleration, velocity, and displacement. The maximum displacement values were obtained from the top story responses of the building model, evaluated through non-linear time history analysis using three earthquake records: Chi-Chi, Kobe, and Superstition Hills. In this study, the IDA procedure applied incremental scale factors of 0.2, which were used to identify the peak displacements in both the x and y directions, as summarized in Table 5.

Table 5. Displacement due to earthquakes

Type of Earthquake	Scale Factor	Max. Displ. X-dir. (mm)	Max. Displ. Y-dir. (mm)
Chichi	0.20	1.781	1.674
Chichi	0.40	3.563	3.348
Chichi	0.60	5.344	5.023
Chichi	0.80	7.126	6.697
Chichi	1.00	8.907	8.371
Chichi	1.20	10.689	10.045
Chichi	1.40	12.470	11.719
Chichi	1.60	14.252	13.394
Chichi	1.80	16.033	15.068
Chichi	2.00	17.815	16.742
Kobe	0.20	2.225	2.203
Kobe	0.40	4.511	4.407
Kobe	0.60	6.766	6.610
Kobe	0.80	9.021	8.814
Kobe	1.00	11.276	11.017
Kobe	1.20	13.532	13.220
Kobe	1.40	15.787	15.424
Kobe	1.60	18.042	17.627
Kobe	1.80	20.298	19.831
Kobe	2.00	22.553	22.034
Superstition Hills	0.20	4.516	2.669
Superstition Hills	0.40	9.032	5.337
Superstition Hills	0.60	13.549	8.006
Superstition Hills	0.80	18.065	10.675
Superstition Hills	1.00	22.581	13.344
Superstition Hills	1.20	27.097	16.012
Superstition Hills	1.40	31.613	18.681
Superstition Hills	1.60	36.130	21.350
Superstition Hills	1.80	40.646	24.019
Superstition Hills	2.00	45.162	26.687

The maximum displacement values in Table 5 can be further used to determine the drift ratio (%) and intensity measure (PGA (g)) as variables for the IDA curve. The determination of damage thresholds was carried out with reference to the ATC-40 guidelines [22], as illustrated in Fig. 7.

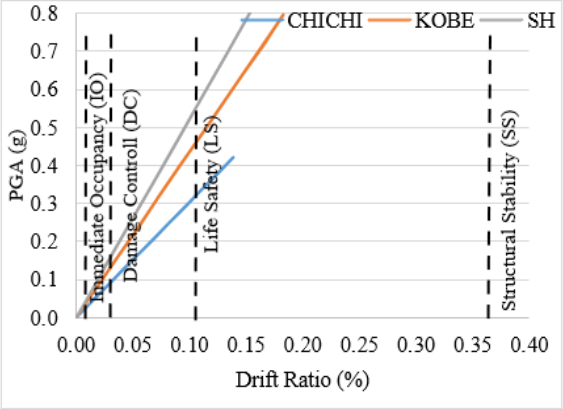

Fig.7 IDA curves

.

4.2 Result of Seismic Fragility Curves

From the structural analysis conducted with the IDA method and applying Eqs. (1–4), the parameters required to construct fragility curves at different levels of damage were obtained, as presented in Table 6. Referring to the data in Table 6, the probability of structural damage was derived and represented in the fragility curve of the evacuation building in Padang City, as illustrated in Fig. 8.

Table 6. Seismic fragility curve parameters

Type Earthquake	Slight PGA (g)	Moderate PGA (g)	Extensive PGA (g)	Complete PGA (g)
CHICHI	0.045	0.085	0.516	1.481
KOBE	0.047	0.088	0.535	1.535
SH	0.052	0.099	0.599	1.720
Total	0.14	0.27	1.65	4.74
N	3	3	3	3
σ	0.004	0.007	0.044	0.125
μ	0.048	0.091	0.550	1.579
ν	0.079	0.079	0.079	0.079
Θ	0.048	0.091	0.548	1.574
β	0.079	0.079	0.079	0.079

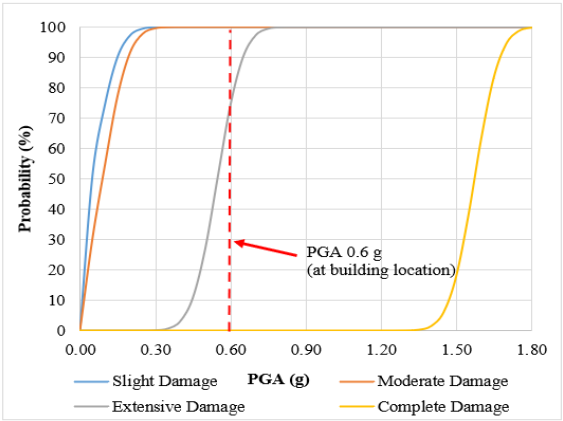

Fig.8 Seismic fragility curves

The use of fragility curves provides a straightforward approach for predicting the potential failure of a structure under future earthquakes. The main requirement is estimating the expected intensity of ground motion. For example, if a future event is assumed to produce a Peak Ground Acceleration (PGA) of 0.6 g, as indicated in the Maximum Considered Earthquake Geometric mean (MCEG) map from SNI 1726:2019, the seismic fragility curve can be applied for evaluation. As shown in Fig. 8, the results indicate a sequential probability pattern: the likelihood of slight and moderate damage reaches 100%, extensive damage has a probability of 74%, while the chance of total collapse is negligible at this PGA level.

4.3 Result of Tsunami Fragility Curves

Using the maximum displacement values obtained from the combined tsunami load analysis and applying Eqs. (8–11), the tsunami fragility curve was developed. This curve was generated by relating structural displacements to different tsunami inundation depths, with the damage state thresholds defined according to the Hazus criteria [24], as presented in Table 7. The corresponding parameters used for constructing the tsunami fragility curve are summarized in Table 8. Referring to the values in Table 8, the tsunami fragility curve for the evacuation building was derived and is presented in Fig. 9.

Table 7. Maximum displacement due to tsunami forces

Tsunami inundation height (m)	Maximum Displ. (mm)	Drift (%)	Damage State
1	0.739	0.006	Slight
2	1.921	0.016	Slight
3	19.071	0.159	Moderate
4	45.237	0.377	Moderate
5	93.182	0.777	Extensive
6	174.276	1.452	Complete
7	287.324	2.394	Complete

Table 8. Parameter of the tsunami fragility curve

Parameter	Slight (m)	Moderate (m)	Extensive (m)	Complete (m)
σ	2.795	3.464	5.025	8.594
μ	2.795	3.464	5.025	8.594
v	1	1	1	1
Θ	1.977	2.450	3.554	6.077
β	0.833	0.833	0.833	0.833

The tsunami fragility curve serves as a tool to estimate the potential levels of structural damage that occur by assuming the height of the tsunami inundation that will occur in the future, based on the tsunami inundation height in the tsunami risk map of Padang City at 5 m. As illustrated in Fig. 9, at a tsunami inundation depth of 5 m in Padang City, the tsunami fragility curves indicate that the probabilities of reaching slight and moderate damage states are certain (100%), while the likelihood of extensive damage escalates to 96%. Furthermore, the building exhibits approximately a 10% probability of undergoing complete structural failure.

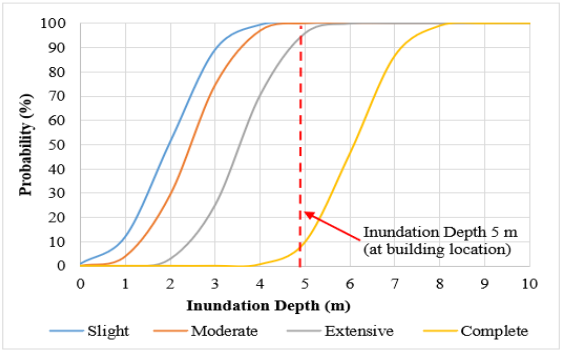

Fig.9 Tsunami fragility curves

5 CONCLUSIONS

The findings of this research indicate that the seismic fragility curve of the SDN 23 school building displays a different probability pattern at a PGA of 0.6 g, where the likelihood of slight and moderate damage reaches 100%, extensive damage is about 74%, and the probability of collapse is negligible. In contrast, the tsunami fragility curve of the building reveals that at an inundation depth of 5 m in Padang City, the chances of slight and moderate damage are certain, extensive damage reaches 96%, and the probability of complete structural failure is approximately 10%.

6 ACKNOWLEDGEMENT

The authors gratefully acknowledge the financial support provided by Universitas Andalas Riset Kolaborasi Indonesia (RKI) Skema C (Host) (Contract No.: 9/UN16.19/PT.01.03/RKI/2024).

7 REFERENCES

1. National Center for Earthquake Studies, Source and Hazard Map of the 2017 Indonesian Earthquake. Ministry of Public Works and Housing (PUPR), Bandung, Indonesia, 2019.
2. Verstappen, H., Indonesian Landforms and Plate Tectonics. Indonesian Journal on Geoscience, Vol. 5, Issue 3, 2010, pp. 197–207. https://doi.org/10.17014/ijog.5.3.197-207.
3. Bambang, B., Examples of Earthquake-Resistant

Building Designs. Institut Teknologi Bandung (ITB), Bandung, Indonesia, 2017.
4. Oktiari, D., and Manurung, S., Geospatial Model of Potential Tsunami Vulnerability in Padang City. Meteorology, Climatology, and Geophysics Agency (BMKG), Padang, Indonesia, 2010, pp. 1–11.
5. Intan, S.U., The Effect of Tsunami Load on the New DPRD Building for the Province of West Sumatra. Andalas University (UNAND), Padang, Indonesia, 2017.
6. Fauzan, Kurniawan, R., Syahdiza, N., Jauhari, Z.A., and Nugraha, D.A., Fragility Curve of School Buildings in Padang City with and without Retrofitting Due to Earthquake and Tsunami Loads. Int. Journal of GEOMATE, Vol. 24, Issue 101, 2023, pp. 102–109. https://doi.org/10.21660/2023.101.g12251.
7. Juliafad, E., and Gokon, H., Seismic Fragility Function for Single-Storey Masonry Wall RC Buildings in Padang City, Indonesia. International Journal of GEOMATE, Vol. 94, Issue 94, 2022, pp. 39–46. https://doi.org/10.21660/2022.94.3160.
8. Ophiyandri, T., Istijono, B., Hidayat, B., and Yunanda, R., Readiness Analysis of Public Buildings in Padang City for Tsunami Temporary Evacuation Shelters. International Journal of GEOMATE, Vol. 22, Issue 94, 2022, pp. 113–120. https://doi.org/10.21660/2022.94.j2391.
9. Fujita, K., and Yashiro, H., Study on Evaluation of Human Damage from Tsunami Considered Congestion of Evacuee. International Journal of GEOMATE, Vol. 22, Issue 89, 2022, pp. 87–93. https://doi.org/10.21660/2022.89.gxi363.
10. Fauzan, Ismail, F.A., Siregar, N., and Jauhari, Z.A., Effect of Tsunami Loads on Pasar Raya Inpres Block III Building in Padang City Based on FEMA P-646. MATEC Web of Conferences, Vol. 258, 2019, Article No. 03020, pp. 1–9. https://doi.org/10.1051/matecconf/201925803020
11. Fauzan, Ismail, F.A., Husna, A.E., Jauhari, Z.A., and Silvia, Effect of Tsunami Loads on Ulak Karang Shelter Building in Padang City. International Journal of Trend in Scientific Research and Development, 2018, pp. 165–173. https://doi.org/10.31142/ijtsrd19130.
12. Frananda, H., Yulianda, F., Boer, M., and Nurjaya, I.W., Coastal Ecology-Based Management for Tsunami Mitigation in Padang City, West Sumatra, Indonesia. Aquaculture, Aquarium, Conservation and Legislation (AACL) Bioflux, Vol. 16, Issue 4, 2023, pp. 2072–2080.
13. Badrul, M., Location of Potential Tsunami Sources in West Sumatra. Jurnal Ilmu Fisika (JIF), Vol. 2, Issue 2, 2010, pp. 94–100.
14. Indonesian National Standardization Agency (BSN), SNI 1727:2020 Minimum Load for Planning of Buildings and Other Structures. Jakarta, Indonesia, 2020, pp. 1–302.
15. Indonesian National Standardization Agency (BSN), SNI 1726:2019 Seismic Resistance Design Codes for Building and Other Structures, BSN, Jakarta, 2019, pp.1-238.
16. Applied Technology Council, FEMA P-646: Guidelines for Design of Structures for Vertical Evacuation from Tsunami. ATC for Federal Emergency Management Agency (FEMA), Redwood City, CA, USA, 2019.
17. Fauzan, Ikhwan, F.M., Nugraha, D.A.M., Syandriadji, D., and Jauhari, Z.A., Effect of Tsunami Loads on Prayoga Foreign Language College Building in Padang City, Indonesia. International Journal of GEOMATE, Vol. 25, Issue 112, 2023, pp. 115–122. https://doi.org/10.21660/2023.112.s8624.
18. Tiwari, V., and Kasnale, A., Incremental Dynamic Analysis of Reinforced Concrete Frames. International Research Journal of Engineering and Technology (IRJET), Vol. 4, Issue 6, 2017, pp. 697–700.
19. Federal Emergency Management Agency (FEMA), HAZUS: Earthquake Loss Estimation Methodology. Washington, D.C., USA, 2002, pp. 11–21.
20. Federal Emergency Management Agency (FEMA), HAZUS Tsunami Model Technical Guidance. Washington, D.C., USA, 2017, pp. 1–171.
21. Janpila, A., Foytong, P., Tirapat, S., and Thanasisathit, N., The Optimal Method for Building Damage Fragility Curve Development. International Journal of GEOMATE, Vol. 18, Issue 69, 2020, pp. 74–80. https://doi.org/10.21660/2020.69.9192.
22. Applied Technology Council, ATC-40: Seismic Evaluation and Retrofit of Concrete Buildings, Vol. 1. Redwood City, CA, USA, 1996, pp. 1–346.
23. Porter, K., A Beginner's Guide to Fragility, Vulnerability, and Risk. University of Colorado Boulder and SPA Risk LLC, Denver, CO, USA, 2021, pp. 2–9.
24. Federal Emergency Management Agency (FEMA), Direct Physical Damage—General Building Stock. HAZUS-MH Technical Manual, Chapter 5, Washington, D.C., USA, 2004.